High-Performance Flexible ZnO Thin-Film Transistors by Atomic Layer Deposition

Mengfei Wang, Xuefei Li, Xiong Xiong, Jian Song, Chengru Gu, Dan Zhan, Qianlan Hu, Shengman Li, and Yanqing Wu

***Abstract*— Flexible zinc oxide thin film transistors (ZnO TFTs) with a mobility of 13 $cm^2/V \cdot s$ and an I_{on}/I_{off} ratio of 1.5×10^8 have been fabricated on polyimide substrate, where the ZnO channel is deposited by atomic layer deposition (ALD) at 140 °C. High bending stability has been achieved due to excellent interface quality between alumina (Al_2O_3) dielectric and ZnO channel with a sharp interface topography. The flexible ZnO device exhibits excellent electrical characteristics even after being bent for 200 000 cycles with a tensile strain of 0.63%. Electrical measurement under a high tensile strain of 2.08% has also been carried out. Moreover, the electrical performance dependence of flexible ZnO TFTs with a tensile strain of 0.78% on temperature from 20 °C to 140 °C has been investigated for the first time.**

***Index Terms*— Flexible ZnO TFTs, ALD, bending stability, NBS/PBS, high temperature.**

I. Introduction

ZINC oxide thin film transistors (ZnO TFTs) fabricated on flexible substrate have attracted great interest such as in wearable electronic equipment and flexible panel displays [1]. ZnO has many advantages over amorphous silicon or organic semiconductors, such as high transparency, high mobility, high long-term reliability, and low cost for large-scale fabrication [2], [3]. Much work has been undertaken to explore the application of ZnO in flexible TFTs. High mobility and bending stability are the key metrics for flexible electronics. Flexible ZnO TFTs fabricated by pulsed laser deposition or sputtering usually exhibit high mobility but low strain tolerance [4]–[9], while those fabricated by solution or printing methods exhibit high strain tolerance but suffer from low mobility [10]–[14]. On the other hand, atomic layer deposition (ALD) has apparent advantages in depositing conformal large-area and high-quality materials at a low temperature, which promises to achieve high mobility and good bending stability [15]–[23].

In practical applications, the operating temperature of flexible TFTs would gradually increase with the working time. Changes in temperature would affect the electrical performance of flexible TFTs [11], [24], [25], thus having a significant effect on the operational performance of wearable electronic equipment or display characteristics of flexible panels. To date, there has been a limited study on the electrical performance dependence of flexible ZnO TFTs under a bending state on temperature.

In this work, flexible ZnO TFTs were fabricated using ALD technique to maximize the quality of materials. The device exhibits a high mobility and a high I_{on}/I_{off} ratio. The improved bending stability is obtained due to the excellent interface quality between Al_2O_3 and ZnO. Moreover, the performance dependence of the bent device on temperature has been investigated for the first time.

II. Device Fabrication

The top panel of Fig. 1a shows the schematic view of a flexible ZnO TFT. The device was fabricated using standard fabrication processes including photolithography and e-beam evaporation. A 20 nm Ni and 60 nm Au metal stack as gate electrode was deposited on a 125 μm polyimide substrate covered with a 100 nm Si_3N_4 buffer layer. Then the substrate was exposed to a mixed plasma of argon and oxygen with a power of 30 W for 30 minutes to remove organic residues. 17 nm Al_2O_3 was deposited by ALD at 140 °C using trimethylaluminum and deionized water. Then the substrate was transferred to glovebox and the chamber was cleaned by pumping the residues for 10 minutes. Next, 10 nm thick ZnO was deposited by ALD at 140 °C using diethylzinc and deionized water. Pulse times were 0.2 and 0.2 s, respectively, and purge times were 7 and 25 s, respectively. Pure N_2 (99.999%) was used as carrier and purge gases. The ZnO channel area with a width of 20 μm and a length of 2 μm was patterned by wet etching with diluted hydrochloric acid. Lastly, a 20 nm Ni and 60 nm Au metal stack was deposited as source and drain electrodes. The bottom figure of Fig. 1a shows the optical image of a flexible sample.

The scanning electron microscopy (SEM) image of the device is shown as Fig. 1b. The high-resolution transmission electron microscopy (HRTEM) and high-angle annular dark field (HAADF) microscopy images in Fig. 1c clearly show the

Manuscript received January 6, 2019; revised January 21, 2019; accepted January 22, 2019. Date of publication January 29, 2019; date of current version March 6, 2019. This work was supported in part by the National Natural Science Foundation of China under Grants 61574066 and 61874162 and in part by the Key Basic Research Program of Hubei Province under Grant 2017AAA127. The review of this letter was arranged by Editor S. Hall. *(Corresponding author: Yanqing Wu.)*

The authors are with the Wuhan National High Magnetic Field Center, Huazhong University of Science and Technology, Wuhan 430074, China, and also with the School of Optical and Electronic Information, Huazhong University of Science and Technology, Wuhan 430074, China (e-mail: yqwu@mail.hust.edu.cn).

Color versions of one or more of the figures in this letter are available online at http://ieeexplore.ieee.org.

Digital Object Identifier 10.1109/LED.2019.2895864

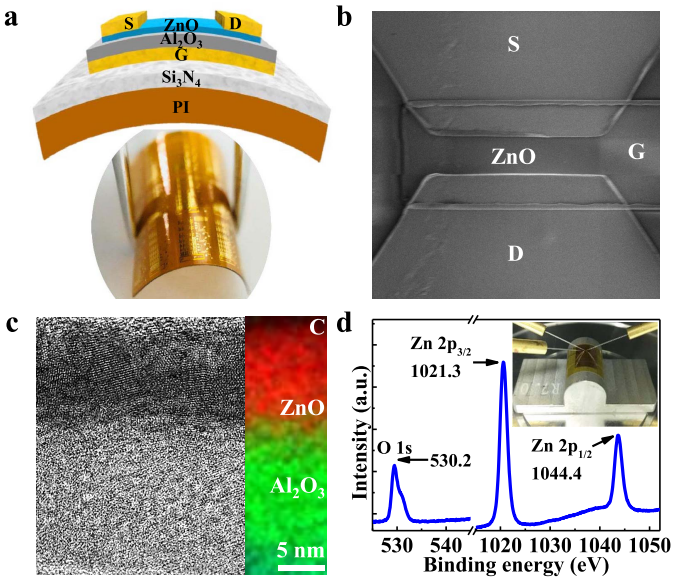

Fig. 1. (a) Top: schematic of the flexible ZnO TFT, bottom: optical image of a flexible sample. (b) SEM image of the device. (c) HRTEM and HAADF images of Al_2O_3 dielectric and ZnO channel. Scale bar: 5 nm. (d) XPS spectrum in O 1s and Zn 2p regions, the insert is a flexible sample attached to an aluminum cylinder.

amorphous structure of Al_2O_3, the polycrystalline structure of ZnO, and a sharp interface. The X-ray photoelectron spectroscopy (XPS) spectrum in Fig. 1d show the O 1s peak at 530.2 eV and Zn 2p spin-orbital splitting doublet with the $2p_{3/2}$ peak at 1021.3 eV and the $2p_{1/2}$ peak at 1044.4 eV [26]. Electrical measurements were carried out using an Agilent parameter analyzer B1500A and a custom-built bending apparatus.

III. Result and Discussion

As shown in the transfer and output characteristics in Fig. 2a and 2b, the as-fabricated device exhibits typical characteristics including an I_{on}/I_{off} ratio of 1.5×10^8, a threshold voltage (V_{th}, extracted using standard method by plotting square root of I_d versus V_g) of 4.39 V, a field effect mobility (μ_{FE}) of 13 $cm^2/V \cdot s$, as well as a maximum drain current (I_{dmax}, normalized by the channel width, defined as the I_d at $V_d = 2$ V and $V_g = 8$ V in output characteristic) of 16.1 μ A/μm, and an on-resistance (R_{on}) of 99.1 $\Omega \cdot$mm. The flexible sample was periodically bent from 0 to 200,000 cycles with a bending direction paralleling to the current flow and a bending radius of 10 mm, corresponding to a tensile strain (ε) of 0.63% [27]. Fig. 2c, d show the dependence of μ_{FE}, V_{th}, I_{dmax}, and R_{on} on the bending cycle, respectively. When the device was bent from 0 to 50,000 cycles, μ_{FE}, V_{th}, I_{dmax}, and R_{on} regularly change for -0.13 $cm^2/V \cdot s$, -0.27 V, 1.1 μA/μm, and -4.2 $\Omega \cdot$ mm, respectively, indicating that the device maintains robust and stable performance. If the device was bent from 50,000 to 200,000 cycles, electrical performance gradually degrades for 32%. After being bent for 200,000 cycles, the device still works well and exhibits characteristics consisting of an I_{on}/I_{off} ratio of 1×10^8, a V_{th} of 4.34 V, a μ_{FE} of 8.9 $cm^2/V \cdot s$, an I_{dmax} of 10.5 μA/μm, and a R_{on} of 150.8 $\Omega \cdot$ mm.

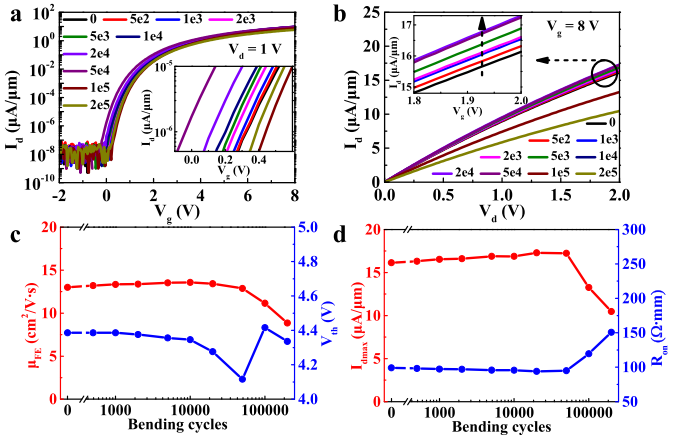

Fig. 2. (a) Transfer characteristics and (b) output characteristics as a function of bending cycle from 0 to 200,000, respectively. Bending radius is fixed at 10 mm. Dependence of (c) μ_{FE}, V_{th}, (d) I_{dmax}, and R_{on} on the bending cycle, respectively.

Fig. 3a and 3b show the electrical performance at different bending radii. The bending radius starts at flat and then changes from 10 to 3 mm in 1 mm step, corresponding to a tensile strain of 0 and 0.63% to 2.08% parallel to the current flow. Fig. 3c, d show the dependence of μ_{FE}, V_{th}, I_{dmax}, and R_{on} on the bending radius, respectively. Excessive strain would do damage to the structure of the device by cracking the layers and interfaces. As the tensile strain increases from 0 to 2.08%, μ_{FE}, V_{th}, I_{dmax}, and R_{on} regularly change for 0.58 $cm^2/V \cdot s$, -0.05 V, -4.6 μA/μm, and 39.4 $\Omega \cdot$mm. The small variations of characteristics under excessive bending cycle or huge tensile strain indicate excellent bending stability of the device, which is due to the excellent interface quality between Al_2O_3 and ZnO. As shown in the benchmark with previous works of bending more than 2,000 cycles in Fig.3e, this is the largest bending cycle under the maximum tensile strain [13], [14], [21], [23]. The tensile strain of 2.09% is the highest value among flexible TFTs with ALD ZnO channel, as shown in Fig. 3f [17], [19]–[21], [23].

The bias-stress stability has also been investigated in the dark. The stress conditions were as follows: $V_g = -2$ V for negative bias stress (NBS), $V_g = 4$ V for positive bias stress (PBS), V_d and $V_s = 0$ V for both. In Fig. 4a and 4b, transfer characteristic shifts negatively and positively respectively for NBS and PBS with a constant subthreshold slope, which excludes the effects of moisture and oxygen in the air [25], [28], [29]. The small V_{th} shifts of -0.16 V for NBS and 0.2 V for PBS after 10,000 s indicate few trapping centers at/near the interface between Al_2O_3 and ZnO [28].

Fig. 5 shows the electrical performance at different temperatures. The sample was bent at a radius of 8 mm all the time, corresponding to a tensile strain of 0.78%. As the temperature and tensile strain application time increase, the oxygen vacancies increase and produce more free electrons, thus causing transfer curves and V_{th} to shift negatively as shown in Fig. 5a, which is also summarized in the right panel of Fig. 5c [24]. Since ZnO layer deposited by ALD has a low impurity concentration, lattice scattering plays a major role as the temperature increases, together with the effect the long-term tensile strain, which results in a decrease in

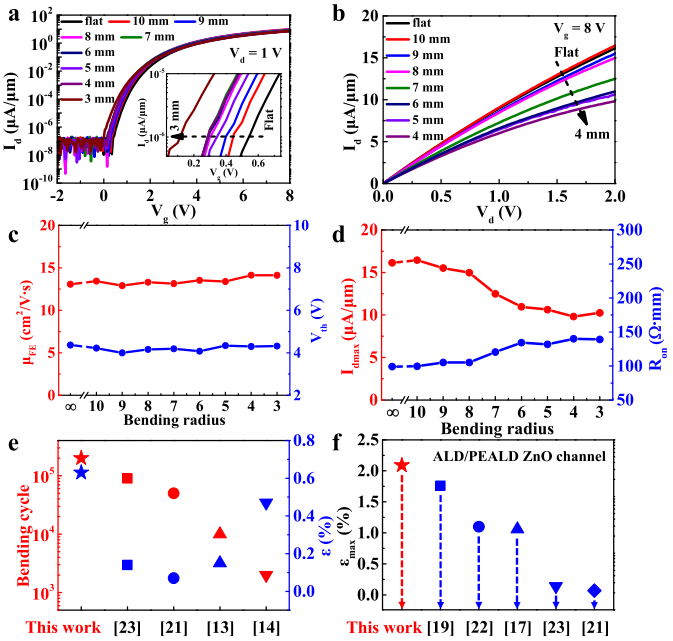

Fig. 3. (a) Transfer characteristics and (b) output characteristics as a function of bending radius, respectively. Dependence of (c) μ_{FE}, V_{th}, (d) I_{dmax}, and R_{on} on the bending radius, respectively. (e) Bending cycles and tensile strain benchmark for different groups' work. (f) Maximum tensile strain benchmark for different groups' work.

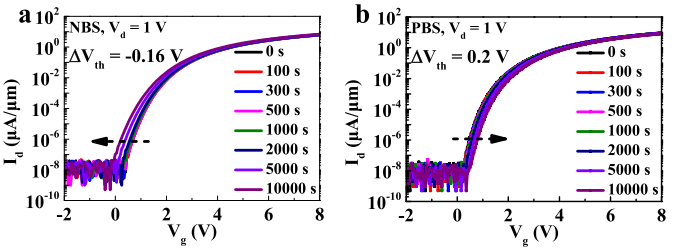

Fig. 4. Transfer characteristics as a function of stress time for (a) NBS and (b) PBS.

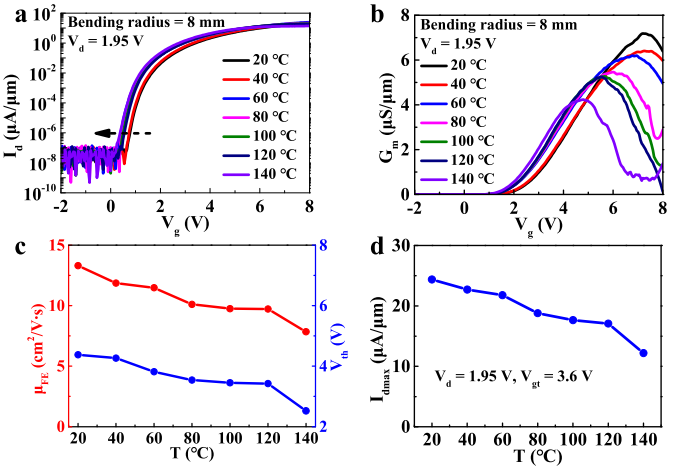

Fig. 5. (a) Transfer characteristics and (b) transconductance as a function of temperature, respectively, V_d = 1.95 V. Dependence of (c) μ_{FE}, V_{th}, and (d) I_{dmax} on the temperature.

transconductance and electron mobility as shown in Fig. 5b and 5c. Fig. 5d shows the dependence of I_{dmax} on the temperature. Where I_{dmax} is defined as the I_d at a fixed V_{gt} ($V_{gt} = V_g - V_{th}$) of 3.6 V and a V_d of 1.95 V in transfer characteristics. With the same carrier concentration at the same V_{gt}, the conductivity decreases with the mobility, causing the current to decrease gradually.

IV. Conclusion

We have demonstrated the fabrication of high-performance flexible ZnO TFTs on the polyimide substrate using low-temperature ALD technique. The device exhibits a μ_{FE} of 13 $cm^2/V \cdot s$ and an I_{on}/I_{off} ratio of 1.5×10^8. Sharp interface topography and decent interface quality based on ALD technique lead to strong electrical stability under different conditions. Detailed electrical characteristics for the flexible ZnO device with 200,000 bending cycles at a tensile strain of 0.63% have been carried out as well as at different bending radius with tensile strain up to 2.08%. The variations of electrical performance with a constant tensile strain of 0.78% at a changing temperature from 20 to 140 °C have been investigated for the first time. These results indicate the potential of ALD ZnO TFTs for flexible electronics.

References

[1] E. Fortunato, P. Barquinha, and R. Martins, "Oxide semiconductor thin-film transistors: A review of recent advances," *Adv. Mater.*, vol. 24, no. 22, pp. 2945–2986, May 2012. doi: 10.1002/adma.201103228.

[2] E. M. C. Fortunato, P. M. C. Barquinha, A. C. M. B. G. Pimentel, A. M. F. Gonçalves, A. J. S. Marques, R. F. P. Martins, and L. M. N. Pereira, "Wide-bandgap high-mobility ZnO thin-film transistors produced at room temperature," *Appl. Phys. Lett.*, vol. 85, no. 13, pp. 2541–2543, Sep. 2004. doi: 10.1063/1.1790587.

[3] K. Nomura, H. Ohta, A. Takagi, T. Kamiya, M. Hirano, and H. Hosono, "Room-temperature fabrication of transparent flexible thin-film transistors using amorphous oxide semiconductors," *Nature*, vol. 432, no. 7016, pp. 488–492, Nov. 2004. doi: 10.1038/nature03090.

[4] C. C. Liu, M. L. Wu, K. C. Liu, S.-H. Hsiao, Y. S. Chen, G.-R. Lin, and J. Huang, "Transparent ZnO thin-film transistors on glass and plastic substrates using post-sputtering oxygen passivation," *J. Display Technol.*, vol. 5, no. 6, pp. 192–197, Jun. 2009. doi: 10.1109/JDT.2008.2009321.

[5] L.-W. Ji, C.-Z. Wu, T.-H. Fang, Y.-J. Hsiao, T.-H. Meen, W. Water, Z.-W. Chiu, and K.-T. Lam, "Characteristics of flexible thin-film transistors with ZnO channels," *IEEE Sensors J.*, vol. 13, no. 12, pp. 4940–4943, Dec. 2013. doi: 10.1109/JSEN.2013.2267808.

[6] S. Park, K. Cho, K. Yang, and S. Kim, "Electrical characteristics of flexible ZnO thin-film transistors annealed by microwave irradiation," *J. Vac. Sci. Technol. B*, vol. 32, no. 6, Nov. 2014, Art. no. 062203. doi: 10.1116/1.4898115.

[7] Y. Zhang, Z. Mei, S. Cui, H. Liang, Y. Liu, and X. Du, "Flexible transparent field-effect diodes fabricated at low-temperature with all-oxide materials," *Adv. Electron. Mater.*, vol. 2, no. 5, Mar. 2016, Art. no. 1500486. doi: 10.1002/aelm.201500486.

[8] Y.-S. Li, J.-C. He, S.-M. Hsu, C.-C. Lee, D.-Y. Su, F.-Y. Tsai, and I.-C. Cheng, "Flexible complementary oxide–semiconductor-based circuits employing n-channel ZnO and p-channel SnO thin-film transistors," *IEEE Electron Device Lett.*, vol. 37, no. 1, pp. 46–49, Jan. 2016. doi: 10.1109/LED.2015.2501843.

[9] R. R. Ghimire and A. K. Raychaudhuri, "High performance thin film transistor (flex-TFT) with textured nanostructure ZnO film channel fabricated by exploiting electric double layer gate insulator," *Appl. Phys. Lett.*, vol. 110, no. 5, Jan. 2017, Art. no. 052105. doi: 10.1063/1.4975209.

[10] K. Song, J. Noh, T. Jun, Y. Jung, H.-Y. Kang, and J. Moon, "Fully flexible solution-deposited ZnO thin-film transistors," *Adv. Mater.*, vol. 22, no. 38, pp. 4308–4312, Aug. 2010. doi: 10.1002/adma.201002163.

[11] Y. Jung, W. Yang, C. Y. Koo, K. Song, and J. Moon, "High performance and high stability low temperature aqueous solution-derived Li–Zr co-doped ZnO thin film transistors," *J. Mater. Chem.*, vol. 22, no. 12, pp. 5390–5397, Feb. 2012. doi: 10.1039/C2JM15526E.

[12] K. Hong, S. H. Kim, K. H. Lee, and C. D. Frisbie, "Printed, sub-2V ZnO electrolyte gated transistors and inverters on plastic," *Adv. Mater.*, vol. 25, no. 25, pp. 3413–3418, Mar. 2013. doi: 10.1002/adma.201300211.

[13] S. H. Kim, J. Yoon, S. O. Yun, Y. Hwang, H. S. Jang, and H. C. Ko, "Ultrathin sticker-type ZnO thin film transistors formed by transfer printing via topological confinement of water-soluble sacrificial polymer in dimple structure," *Adv. Funct. Mater.*, vol. 23, no. 11, pp. 1375–1382, Mar. 2012, doi: 10.1002/adfm.201202409.

[14] K. T. Eun, W. J. Hwang, B. K. Sharma, J. H. Ahn, Y. K. Lee, and S. H. Choa, "Mechanical flexibility of zinc oxide thin-film transistors prepared by transfer printing method," *Mod. Phys. Lett. B*, vol. 26, no. 12, May 2012, Art. no. 1250077. doi: 10.1142/S0217984912500777.

[15] X. Xiong, X. Li, M. Huang, T. Li, T. Gao, and Y. Wu, "High performance black phosphorus electronic and photonic devices with HfLaO dielectric," *IEEE Electron Device Lett.*, vol. 39, no. 1, pp. 127–130, Jan. 2018. doi: 10.1109/LED.2017.2779877.

[16] D. A. Mourey, D. A. Zhao, and T. N. Jackson, "ZnO thin film transistors and circuits on glass and polyimide by low-temperature PEALD," in *IEDM Tech. Dig.*, Dec. 2009, pp. 1–4. doi: 10.1109/IEDM.2009.5424388.

[17] K. H. Cherenack, N. S. Munzenrieder, and G. Troster, "Impact of mechanical bending on ZnO and IGZO thin-film transistors," *IEEE Electron Device Lett.*, vol. 31, no. 11, pp. 1254–1256, Nov. 2010, doi: 10.1109/led.2010.2068535.

[18] D. Zhao, D. A. Mourey, and T. N. Jackson, "Fast flexible plastic substrate ZnO circuits," *IEEE Electron Device Lett.*, vol. 31, no. 4, pp. 323–325, Apr. 2010. doi: 10.1109/led.2010.2041321.

[19] J.-M. Kim, T. Nam, S. J. Lim, Y. G. Seol, N.-E. Lee, D. Kim, and H. Kim, "Atomic layer deposition ZnO:N flexible thin film transistors and the effects of bending on device properties," *Appl. Phys. Lett.*, vol. 98, no. 14, Apr. 2011, Art. no. 142113. doi: 10.1063/1.3577607.

[20] Y.-Y. Lin, C.-C. Hsu, M.-H. Tseng, J.-J. Shyue, and F.-Y. Tsai, "Stable and high-performance flexible ZnO thin-film transistors by atomic layer deposition," *ACS Appl. Mater. Interfaces*, vol. 7, no. 40, pp. 22610–22617, Oct. 2015. doi: 10.1021/acsami.5b07278.

[21] H. U. Li and T. N. Jackson, "Oxide semiconductor thin film transistors on thin solution-cast flexible substrates," *IEEE Electron Device Lett.*, vol. 36, no. 1, pp. 35–37, Jan. 2015, doi: 10.1109/led.2014.2371011.

[22] Y. Afsar, J. Tang, W. Rieutort-Louis, L. Huang, Y. Hu, J. Sanz-Robinson, N. Verma, S. Wagner, and J. C. Sturm, "Impact of bending on flexible metal oxide TFTs and oscillator circuits," *J. Soc. Inf. Display*, vol. 24, no. 6, pp. 371–380, May 2016. doi: 10.1002/jsid.445.

[23] H. U. Li and T. N. Jackson, "Flexibility testing strategies and apparatus for flexible electronics," *IEEE Trans. Electron Devices*, vol. 63, no. 5, pp. 1934–1939, May 2016. doi: 10.1109/TED.2016.2545706.

[24] K. Takechi, M. Nakata, T. Eguchi, H. Yamaguchi, and S. Kaneko, "Temperature-dependent transfer characteristics of amorphous $InGaZnO_4$ thin-film transistors," *Jpn. J. Appl. Phys.*, vol. 48, no. 1R, Jan. 2009, Art. no. 011301. doi: 10.1143/jjap.48.011301.

[25] P. K. Nayak, Z. Wang, and H. N. Alshareef, "Indium-free fully transparent electronics deposited entirely by atomic layer deposition," *Adv. Mater.*, vol. 28, no. 35, pp. 7736–7744, Sep. 2016, doi: 10.1002/adma.201600503.

[26] P.-T. Hsieh, Y.-C. Chen, K.-S. Kao, and C.-M. Wang, "Luminescence mechanism of ZnO thin film investigated by XPS measurement," *Appl. Phys. A, Solids Surf.*, vol. 90, no. 2, pp. 317–321, Feb. 2008. doi: 10.1007/s00339-007-4275-3.

[27] H. Gleskova, S. Wagner, and Z. Suo, "a-Si:H thin film transistors after very high strain," *J. Non-Crystalline Solids*, vols. 266–269, pp. 1320–1324, May 2000. doi: 10.1016/S0022-3093(99)00944-8.

[28] M. E. Lopes, H. L. Gomes, M. C. R. Medeiros, P. Barquinha, L. Pereira, E. Fortunato, R. Martins, and I. Ferreira, "Gate-bias stress in amorphous oxide semiconductors thin-film transistors," *Appl. Phys. Lett.*, vol. 95, no. 6, Aug. 2009, Art. no. 063502. doi: 10.1063/1.3187532.

[29] P. K. Nayak, J. V. Pinto, G. Goncalves, R. Martins, and E. Fortunato, "Environmental, optical, and electrical stability study of solution-processed zinc–tin–oxide thin-film transistors," *J. Display Technol.*, vol. 7, no. 12, pp. 640–643, Dec. 2011. doi: 10.1109/JDT.2011.2160151.